UNIVERSY OF SEVILLE

Faculty of Physics

Department of Atomic, Molecular and Nuclear Physics

FOUNDATIONS OF QUANTUM COMPUTING AND ITS IMPLEMENTATION IN TRAPPED IONS

JESÚS GERARDO PAREJO GONZÁLEZ

Tutor: **DR LUCAS LAMATA MANUEL**

Seville, Spain
2021

Index

1 Introduction

Since the development, in 1943, of the first completely functional computer (ENIAC), classical computers have been establishing a before and after in data treatment of many science fields. Although its computing potential is rising exponentially, the most essential operation in a computer is the control of an electric pulse in order to create bits. In this context, the existence of this pulse is understood as "1" and the absence of it as "0". This creates a physical limitation of the performing of classical computers. The efficiency of current hardware relies in the increase of the density of transistors.

Furthermore, in 1900s, quantum mechanics (QM) emerges. This is a physical theory which can describe properly the microscopical reality. QM explained some phenomena unobserved at macroscopic scales.

In 1970s decade, some computer and information scientists tried to combine QM with information science in order to design and manipulate a quantum system. This idea subsequently introduced quantum technology field, in which quantum computers are proposed and studied. Nevertheless, at this point, classical computers had excellent performance. Thus, it was necessary to prove that the quantum ones could give an advantage.

The first time, theoretically, that a quantum computer could overcome a classical one in the resolution of a task was shown by Peter Shor with his well-known factoring quantum algorithm **[1]**. Shor's factoring algorithm is a quantum algorithm for factoring a number N in a polynomial time. It has implications in cryptography and was a motivation for increasing the interest in this field.

This incentive is translated in a two-decade of investigations and attempts of implementing these ideas in physical systems. Best candidates to perform quantum computing are superconductors, optical lattices, trapped ions, as well as nuclear magnetic resonances, among others. We will focus in the trapped-ion quantum computer paradigm.

The field of quantum technologies has led, most notably, to the development of quantum computers, which permit the study of systems (generally of a quantum nature) that cannot be simulated via current supercomputers or in the laboratory.

The first chapter of this thesis will provide a presentation to quantum computing, followed by the basic trapped-ion physics formalism. Once we have described both topics, we will discuss how to implement quantum computing concepts into an ion trap.

2 Introduction to quantum computing

Quantum computing (QC) consists in employing quantum devices in order to perform computation and information processing tasks more efficiently than with classical computers. This thesis main aim is to give a review of QC, focusing on the quantum platform of trapped ions.

Let us introduce some helpful mathematical definitions used for QC formalism:

- **Dirac notation (braket notation).** Typically used in QM. It introduces two objects denotated as *"ket"*, $|\cdot\rangle$, abstract and complex elements from a vectorial space $\mathcal{E}$ and *"bra"*, $\langle\cdot|$, linear forms belonging to the dual space $\mathcal{E}^*$. This structure allows one to identify a *"bra-ket"*, $\langle\cdot|\cdot\rangle$, as an inner product which gives $\mathcal{E}$ the properties of a Hilbert space.
- **Operator**. Linear map which converts a ket into a ket. $|\psi\rangle \in \mathcal{E}, \hat{A}|\psi\rangle \in \mathcal{E}$. In our interests, we can understand it as an N x N matrix acting on the states of a system.

In 2000, *David P. DiVincenzo* proposed his criteria enumerating what a physical system should satisfy to be considered as a quantum computer **[2]**.

1. *A scalable physical system with well characterized qubits.*
2. *The ability to initialize the state of the qubits to a simple fiducial state.*
3. *Long relevant decoherence times, much longer than the gate operation time.*
4. *A "universal" set of quantum gates.*
5. *A qubit-specific measurement capability.*
6. *The ability to interconvert stationary and flying qubits.*
7. *The ability to faithfully transmit flying qubits between specified locations.*

2.1 Quantum bits (qubits)

A qubit is defined as a two level quantum system that can be properly modified. In Dirac notation:

$$|\psi\rangle = \alpha|0\rangle + \beta|1\rangle \tag{1}$$

where $\alpha, \beta \in \mathbb{C}$ and $|\alpha|^2$, $|\beta|^2$ are the probabilities of the system to collapse to $|0\rangle$ or $|1\rangle$ respectively. It can be understood as a generalization of a classical bit, which states available are only 0 or 1.

2.1.1 Bloch sphere

The most common representation of a single qubit is the *Bloch sphere*. Applying this description, the qubit state is shown as a point of the surface of a unitary sphere. **[3]**

To express Eq. (1) hereby, we must rewrite α and β in their polar form:

$$\alpha = r_\alpha e^{i\phi_\alpha} \qquad\qquad \beta = r_\beta e^{i\phi_\beta} \tag{2}$$

We obtain:

$$|\psi\rangle = e^{i\phi_\alpha}(r_\alpha |0\rangle + r_\beta e^{i(\phi_\beta - \phi_\alpha)} |1\rangle) \tag{3}$$

The first term in Eq. (3) is a global phase, thus it is unobservable and we omit it. In a quantum state, $\langle\psi|\psi\rangle = 1$. If we rewrite the amplitude of $|1\rangle$ as $r_\beta e^{i(\phi_\beta - \phi_\alpha)} = r_\beta e^{i\phi} = (x + iy)$,

$$\langle\psi|\psi\rangle = r_\alpha^2 + x^2 + y^2 = 1 \tag{4}$$

Eq. (4) is the implicit equation of a sphere of radius 1. We identify $(x, y, r) \to (x, y, z)$. Applying a spherical transformation: $(x, y, z) \to (r = 1, \theta', \phi)$, Eq. (3) takes the form:

$$|\psi\rangle = \cos\theta' |0\rangle + \sin\theta' e^{i\phi} |1\rangle \qquad 0 \leq \theta' \leq \pi/2,\ \ 0 \leq \phi \leq 2\pi \tag{5}$$

However, with this mapping, there only exists half sphere of independent points. It is straightforward to see: $|\psi(\theta' = 0, \phi)\rangle = |0\rangle$ and $|\psi(\theta' = \pi/2, \phi = 0)\rangle = |1\rangle$. In addition, the downside represents the same states as the upper-side: $|\psi'(\pi - \theta', \phi + \pi)\rangle = -|\psi(\theta', \phi)\rangle$.

To fix this problem, we introduce a variable change $\theta = 2\theta'$ turning Eq. (5) into

$$|\psi\rangle = \cos(\theta/2) |0\rangle + \sin(\theta/2) e^{i\phi} |1\rangle \qquad 0 \leq \theta \leq \pi,\ \ 0 \leq \phi \leq 2\pi \tag{6}$$

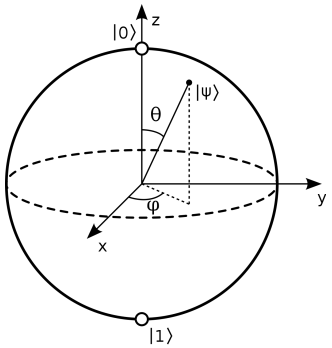

Figure 1: Scheme of a qubit in the Bloch sphere. Source in Ref. [4].

2.1.2 Multiple qubit systems

Beyond a single qubit system, this problem can be generalized to a situation with multiple qubits. In the N-qubit case dimension grows as 2^N. To reach scalable quantum computers a requirement must be to increase the number of qubits.

We can write an N qubit state as (the symbol $\otimes$ denotes the tensor product among all the inner spaces of qubits):

$$|010\ldots0\rangle = |0\rangle_1 \otimes |1\rangle_2 \otimes |0\rangle_3 \otimes \cdots \otimes |0\rangle_N \tag{7}$$

An important application of a two-qubit system is the *Bell state* or *EPR pair*. They permit to create correlated quantum states between qubits, also known as *quantum entanglement*. An example of Bell state is:

$$|\Psi\rangle = \frac{1}{\sqrt{2}}(|00\rangle + |11\rangle) \tag{8}$$

2.2 Quantum logic gates

The way to describe quantum gates (QG) is via unitary operators acting on qubits. In an N-dimensional Hilbert space, an operator can be represented as an $N \times N$ matrix. The only constrains which limit the form of the operators is that they must maintain invariant the norm and be linear. Thus, the operator $\hat{A}$ will be unitary: $\hat{A}^\dagger\hat{A} = \hat{A}\hat{A}^\dagger = \mathbb{I}$

As the system can be found in two orthogonal states when it is measured, $|0\rangle$ and $|1\rangle$ can be written as,

$$|0\rangle \equiv \begin{pmatrix} 1 \\ 0 \end{pmatrix}; \quad |1\rangle \equiv \begin{pmatrix} 0 \\ 1 \end{pmatrix}; \tag{9}$$

In this context, a single qubit gate is represented by a 2×2 matrix. Graphically, it could be understood as rotations of $|\psi\rangle$ around the Bloch sphere [see Fig. (1)]. The single QG can be expressed in terms of Pauli matrices:

$$X \equiv \begin{pmatrix} 0 & 1 \\ 1 & 0 \end{pmatrix}; \quad Y \equiv \begin{pmatrix} 0 & -i \\ i & 0 \end{pmatrix}; \quad Z \equiv \begin{pmatrix} 1 & 0 \\ 0 & -1 \end{pmatrix} \tag{10}$$

and the Hadamard gate, $H = \frac{1}{\sqrt{2}} \begin{pmatrix} 1 & 1 \\ 1 & -1 \end{pmatrix}$

Generalizing, a multiple qubit gate will be interpreted as a $2^N \times 2^N$ matrix, where N is the number of qubits involved.

An important result of theoretical computing is the research of the universality of the NAND gate. Any function can be computed as the proper composition of NAND gates. An

equivalent statement is postulated for QG. A universal gate set is compound of the Controlled-NOT (CNOT) and single qubit gates **[5]**.

2.2.1 CNOT gate

The CNOT gate is a two-qubit gate, with two inputs and two outputs. It has the following matrix elements [see Fig. (2)]:

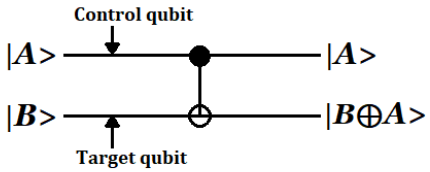

Figure 2: Circuit of a CNOT gate.

In multiple-qubit states, we construct a compound state as the tensor product of the single-qubit states. Employing the representation of Eq. (9), we can create any two-qubit state. An example for clarity purposes would be:

$$|11\rangle = |1\rangle \otimes |1\rangle = \begin{pmatrix} 0 \\ 1 \end{pmatrix} \otimes \begin{pmatrix} 0 \\ 1 \end{pmatrix} = \begin{pmatrix} 0 \cdot \begin{pmatrix} 0 \\ 1 \end{pmatrix} \\ 1 \cdot \begin{pmatrix} 0 \\ 1 \end{pmatrix} \end{pmatrix} = \begin{pmatrix} 0 \\ 0 \\ 0 \\ 1 \end{pmatrix} \tag{11}$$

Thus, employing this notation, its matrix representation is: $U_{CNOT} = \begin{pmatrix} 1 & 0 & 0 & 0 \\ 0 & 1 & 0 & 0 \\ 0 & 0 & 0 & 1 \\ 0 & 0 & 1 & 0 \end{pmatrix}$

This gate has two well differentiated inputs, a control qubit, which produces, when set to zero, that the second qubit (target) remains unaltered. Otherwise, the target flips.

Summarizing, the action of a CNOT gate over two qubits can be described as:

$$|A, B\rangle \longrightarrow |A, B \oplus A\rangle \tag{12}$$

In this case, $\oplus$ is defined as the addition modulo two.

2.3 Quantum algorithms

The fundamental application of qubits and quantum gates is the elaboration of quantum algorithms which improve classical ones, specifically, on the time speedup solving a problem. They can be classified in two groups: *QFT (quantum Fourier transform)* and *quantum searching*.

The first quantum algorithm which overcame the classical protocol was the Deutsch-Jozsa algorithm. Despite solving a trivial problem, it caught the attention of many scientists and contributed to rise quantum computing.

2.3.1 Deutsch-Jozsa algorithm

Problem statement: Given an unknown Boolean function $f : \{0,1\}^n \rightarrow \{0,1\}$, which is guaranteed to be balanced or constant, determine the behaviour of the function.

Classical approach. To have certainty that f is constant, in the worst case, it is necessary to try half plus one combinations. In an n-bits chain, $2^{n-1}+1$ trials.

Quantum solution. In this case, with only one trial we can determine the solution.

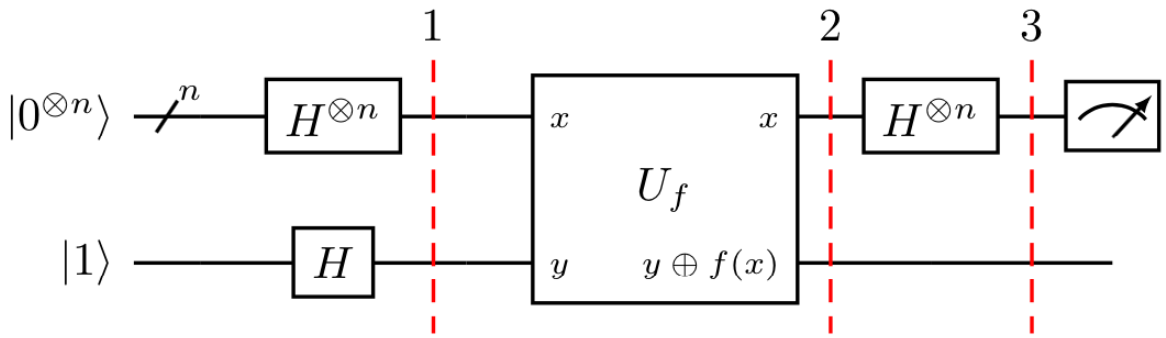

Figure 3: Deutsch-Jozsa's diagram. Source in Ref. **[3]**

The algorithm can be split in three steps, where we have introduced the notation: $|0\rangle^{\otimes n} = \overbrace{|0\ldots0\rangle}^{n-times}$.

The initial state is:

$$|\psi_0\rangle = |0\rangle^{\otimes n} \otimes |1\rangle = |0\ldots01\rangle \tag{13}$$

Applying a Hadamard gate on Eq. (13).

$$|\psi_1\rangle = \frac{1}{\sqrt{2^{n+1}}} \sum_{x=0}^{2^n-1} |x\rangle(|0\rangle - |1\rangle), \tag{14}$$

where we define x as the different possibilities of sorting an n-length chain of 0's and 1's (the last qubit $|1\rangle$ is written explicitly, $H|1\rangle = \frac{1}{\sqrt{2}}(|0\rangle - |1\rangle)$).

The function U_f is called an *oracle*. It behaves like a black box for which only the inputs and outputs are known.

$$|\psi_2\rangle = U_f|\psi_1\rangle = \frac{1}{\sqrt{2^{n+1}}} \sum_{x=0}^{2^n-1} |x\rangle(|f(x)\rangle - |1 \oplus f(x)\rangle) = \frac{1}{\sqrt{2^{n+1}}} \sum_{x=0}^{2^n-1} (-1)^{f(x)}|x\rangle(|0\rangle - |1\rangle) \tag{15}$$

because $f(x) = 0$ or 1, thus: $|f(x)\rangle - |1 \oplus f(x)\rangle = (-1)^{f(x)}(|0\rangle - |1\rangle)$

At this point, let us ignore the last qubit interaction. A second Hadamard gate is applied on the first n-qubits. To simplify the notation, a concise way of writing the action of a Hadamard gate for a single qubit is: $H|x\rangle = \sum_{z=0}^{1}(-1)^{xz}|z\rangle/\sqrt{2}, \quad x = 0, 1.$

$$|\psi_3\rangle = \frac{1}{2^n} \sum_{x=0}^{2^n-1} (-1)^{f(x)} \left[\sum_{y=0}^{2^n-1} (-1)^{x\cdot y}|y\rangle\right] = \frac{1}{2^n} \sum_{y=0}^{2^n-1} \left[\sum_{x=0}^{2^n-1} (-1)^{f(x)+x\cdot y}\right] |y\rangle \tag{16}$$

The last step is to measure $|\psi_3\rangle$. The system will collapse to an eigenstate. If it is returned $|0\rangle^{\otimes n}$ then $f(x)$ is constant and it is balanced otherwise. This is due to the fact that the probability of the system to be in $|0\rangle^{\otimes n}$ is:

$$P(|0\rangle^{\otimes n}) = \left| \frac{1}{\sqrt{2^n}} \sum_{x=0}^{2^n-1} (-1)^{f(x)} \right|^2$$

If $f(x)$ is a balanced function, the quantity of $+1$ is the same as -1. Thus, $|\psi_3\rangle$ cannot collapse to it.

3 Introduction to trapped ions

In this section, we will introduce the basics of what an ion trap is and how it works. Furthermore, we will study a procedure of cooling ions and detecting their state.

3.1 Ion trapping

An ion trap is an isolate system of confined ionized atoms which is set in a well-known state of motion. To achieve this state (and manipulate it later), it is necessary to employ electromagnetic fields. Depending on the kind of field, there exists different ion traps, such as Penning and Paul traps.

Penning traps are designed employing a homogeneous magnetic field and a quadrupole electric field. On the other hand, Paul traps are built of an inhomogeneous time-dependent field, typically oscillating in the rf (radio-frequency) domain. As a result, Paul traps are often named as rf traps.

3.2 Motion of particles in a Paul trap

Since this kind of traps is sometimes used for confining ions for the purpose of employing them as physical qubits, let us describe in detail their complete behaviour.

Initially, it is important to remark Earnshaw's theorem: *a stable stationary equilibrium of a set of charges cannot be maintained by the purely electrostatic interaction of the system*. Due to this result, the electric potential, quadrupolar-shaped, may be decomposed into a static part and a sinusoidal part with an angular frequency ω_{rf}.

$$\Phi(x,y,z,t) = \frac{K}{2}\left(\alpha x^2 + \beta y^2 + \gamma z^2\right) + \frac{K'}{2}\cos\left(\omega_{\mathrm{rf}} t\right)\left(\alpha' x^2 + \beta' y^2 + \gamma' z^2\right) \tag{17}$$

In each point with no particles, this potential has to fulfill Laplace's equation: $\nabla^2\Phi = 0$. Developing the equation:

$$\nabla^2\Phi(x,y,z,t) = K\left(\alpha+\beta+\gamma\right) + K'\cos\left(\omega_{\mathrm{rf}} t\right)\left(\alpha'+\beta'+\gamma'\right) = 0, \quad \forall t \tag{18}$$

it leads to the geometrical relations:

$$\begin{aligned} &\alpha + \beta + \gamma = 0 \\ &\alpha' + \beta' + \gamma' = 0 \end{aligned} \tag{19}$$

Consequently, there are no local minima in the free space that are consistent with Earnshaw's theorem. For instance, a geometrical factor election in which the charge is confined in a

purely rotating field would be:

$$\begin{aligned} \alpha = \beta = \gamma = 0 \\ \alpha' + \beta' = -\gamma' \end{aligned} \tag{20}$$

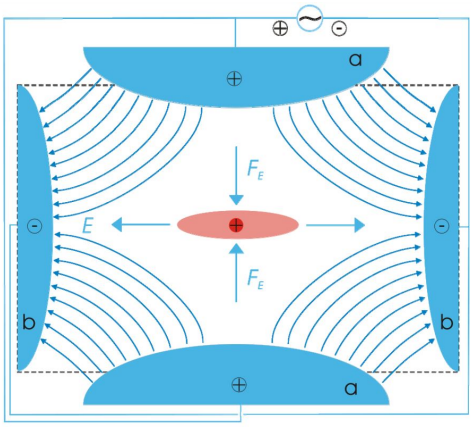

Figure 4: Schematic of a linear ion trap. Source in Ref. **[6]]**.

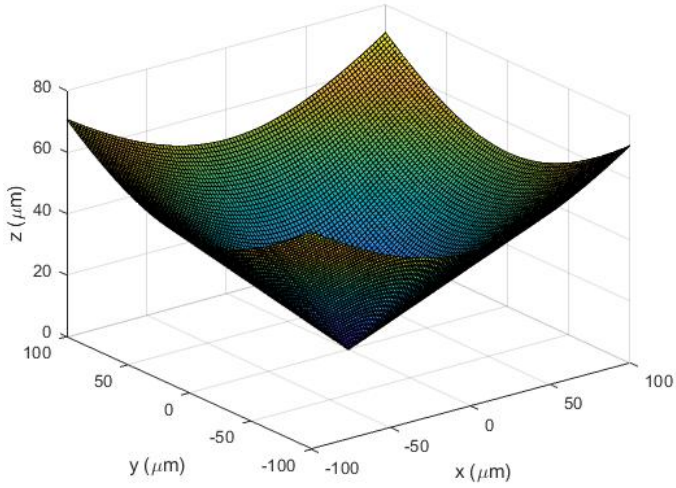

Figure 5: Commonly used static potential well created for an isolated ion. This is represented via an equipotential surface, $\Phi = 0$ of Eq. (17) with the parameter condition $-(\alpha + \beta) = \gamma > 0$. We have chosen $\alpha = \beta = -1$ and a range $0 < |r| < 100$ μm.

In addition, it is important to analyze the motion of ions in rf traps. These traps are of the order of $\sim 1\text{mm} - 1\text{cm}$. Nevertheless, atoms are systems of ~ 1Å, therefore, a quantum-mechanical treatment of the problem may be required. In addition, the potential in Eq. (17) is time-dependent, the most considerable effect of is: $\langle \Phi(x, y, z, t) \rangle \neq \Phi(x, y, z, \langle t \rangle)$. In 1985, Cook, Shankland, and Wells **[7]** developed the first quantum-treatment of a rf trap and concluded that the stability regions of the traps are identical as the classical ones.

Eq. (17) can be rewritten as a separable problem in Cartesian coordinates. Without loss of generality, let us focus in the x-coordinate.

$$V(t) = \frac{1}{2} m W(t) \hat{x}^2 \tag{21}$$

with

$$W(t) = \frac{1}{4} \omega_{\text{rf}}^2 \left[a_x + 2 q_x \cos\left(\omega_{\text{rf}} t\right) \right]. \tag{22}$$

The two new parameters are related to the geometrical factors: $a_x \propto \alpha$ and $q_x \propto \alpha'$.

The motional Hamiltonian is:

$$\hat{H}^{(m)}(t) = K + V(t) = \frac{\hat{p}^2}{2m} + \frac{1}{2}mW(t)\hat{x}^2. \tag{23}$$

In the Heisenberg picture, the time evolution of the operators $\hat{x}$ and $\hat{p}$ follows the expression,

$$\frac{d\hat{A}^H}{dt}(t) = \frac{\partial \hat{A}^H}{\partial t} + \frac{i}{\hbar}[\hat{H}, \hat{A}^H] \tag{24}$$

Thus,

$$\begin{aligned} \dot{\hat{x}} &= \tfrac{\hat{p}}{m}, \\ \dot{\hat{p}} &= -mW(t)\hat{x}. \end{aligned} \tag{25}$$

Coupling both equations,

$$\ddot{\hat{x}} + W(t)\hat{x} = \ddot{\hat{x}} + \frac{1}{4}\omega_{\mathrm{rf}}^2 \left[a_x + 2q_x \cos\left(\omega_{\mathrm{rf}} t\right)\right] \hat{x} = 0. \tag{26}$$

This kind of equation is called *"Mathieu equation"* **[8]**, which has the standard form,

$$u'' + (a - 2q\cos(2\xi))u = 0, \tag{27}$$

and its more general solution is:

$$u(\xi) = Ae^{i\beta_x \xi} \sum_{n=-\infty}^{\infty} C_{2n} e^{i2n\xi} + Be^{-i\beta_x \xi} \sum_{n=-\infty}^{\infty} C_{2n} e^{-i2n\xi}. \tag{28}$$

As a result, if we relate $\hat{x} \to u(t)$, Eq. (26) has the structure of Eq. (27). Imposing the boundary conditions, $\quad u(0) = 1, \quad \dot{u(0)} = i\nu$, the solution can be constructed using Eq. (28) with $A = 1, \quad B = 0$.

$$u(t) = e^{i\beta_x \omega_{\mathrm{rf}}/2} \sum_{n=-\infty}^{\infty} C_{2n} e^{in\omega_{\mathrm{rf}} t} \equiv e^{i\beta_x \omega_{\mathrm{rf}} t/2} \Phi(t). \tag{29}$$

The complex conjugate solution is linearly independent of $u(t)$. It can be shown calculating the Wronskian:

$$\begin{aligned} u^*(t)\dot{u}(t) - u(t)\dot{u}^*(t) =& U^*(t;0)u^*(0)U(t;0)\dot{u}(0) - U(t;0)u(0)U^*(t;0)\dot{u}^*(0) = \\ &= u^*(0)\dot{u}(0) - u(0)\dot{u}^*(0) = 2i\nu. \end{aligned} \tag{30}$$

In this context, $U(t;0)$ is the time evolution operator and $[U(t;0), u(0)] = 0$.

Since the Wronskian is a time constant and $u(t), \hat{x}$ follow the same ODE, multiplying Eq. (30) by a constant and $u^*(t) \to \hat{x}$,

$$\hat{C}(t) = \hat{C}(0) = \sqrt{\frac{m}{2\hbar\nu}} i\{u(t)\dot{\hat{x}}(t) - \dot{u}(t)\hat{x}(t)\} = \frac{1}{\sqrt{2m\hbar\nu}}[m\nu\hat{x}(0) + i\hat{p}(0)] = \hat{a}. \tag{31}$$

From Eq. (31), the Heisenberg position operator can be rewritten in terms of $u(t)$ and its complex conjugate function,

$$\hat{x}(t) = \sqrt{\frac{\hbar}{2m\nu}} \left\{\hat{a}u^*(t) + \hat{a}^\dagger u(t)\right\}. \tag{32}$$

In this context, $\hat{a}$ is the annihilator operator of a harmonic oscillator. As a result, it will satisfy its commutation relations and a basis of the problem will take the form, $|n,t\rangle_\nu, \quad n = 1, ..., \infty$

The ground state obeys,

$$\hat{a}\,|n=0,t\rangle = \sqrt{\frac{m}{2\hbar\nu}}[u(t)\dot{\hat{x}} - \dot{u(t)}\hat{x}] = \sqrt{\frac{m}{2\hbar\nu}}[u(t)\frac{p}{m} - \dot{u(t)}\hat{x}] = 0. \tag{33}$$

Rearranging:

$$[u(t)\frac{p}{m} - \dot{u(t)}\hat{x}] = 0. \tag{34}$$

Moreover, in the coordinate space,

$$\left\{u(t)\frac{\hbar}{i}\frac{\partial}{\partial x} - m\dot{u}(t)x\right\}\langle x \mid n=0,t\rangle = 0. \tag{35}$$

Solving and normalizing Eq. (35),

$$\langle x' \mid n=0,t\rangle = \left(\frac{m\nu}{\pi\hbar}\right)^{1/4} \frac{1}{\{u(t)\}^{1/2}} \exp\left[\frac{im}{2\hbar}\frac{\dot{u}(t)}{u(t)}x'^2\right]. \tag{36}$$

By a similar procedure used in harmonic oscillator, the excited states can be created,

$$|n,t\rangle = \frac{\left[\hat{a}^\dagger(t)\right]^n}{\sqrt{n!}}|n=0,t\rangle = \frac{\left[C^\dagger(t)\right]^n}{\sqrt{n!}}|n=0,t\rangle \tag{37}$$

The essential statement shown in Eq. (37) is that the solutions are coherent states. Consequently, they are not eigenstates of the hamiltonian (there is a periodical exchange between the rf field and the ions) and, eventually, these states will collapse into an eigenstate. As a result, the operation time of the gates acting on the qubits must be shorter than decoherence time.

3.3 Trapped ion Hamiltonian

A further ingredient in trapped ion dynamics is the coupling of electromagnetic fields with the internal and motional states of the ions. It is formally equivalent to the Jaynes-Cummings Hamiltonian.

As a result of the relative strength of the coupling, the interaction with levels distant from the resonance frequency is negligible. The structure is typically approximated by a two-level quantum system. The two levels are denoted by $|g\rangle$, the ground state, and $|e\rangle$, the excited state. The energy between both levels is $\hbar\omega_o = \hbar(\omega_e - \omega_g)$ and the Hamiltonian is:

$$H^{(e)} = \hbar(\omega_g |g\rangle \langle g| + \omega_e |e\rangle \langle e|) \tag{38}$$

By rescaling the energy in Eq. (38) a factor $-\hbar(\omega_e + \omega_g)/2$, the Hamiltonian can be rewritten as:

$$\hat{H}^{(e)} = \hbar\frac{\omega_o}{2}\sigma_z. \tag{39}$$

For a two-level system, operators can be expressed using Pauli matrices assigning $|g\rangle \mapsto (1,0)$ and $|e\rangle \mapsto (0,1)$.

The total Hamiltonian will include the motion of the ions, $\hat{H}^{(m)}$, the internal electronic level, $\hat{H}^{(e)}$ and the interaction with electromagnetic fields, $\hat{H}^{(i)}$.

$$\hat{H} = \hat{H}^{(m)} + \hat{H}^{(e)} + \hat{H}^{(i)} \tag{40}$$

Let us discuss how to deduce the interaction part of the Hamiltonian. The electromagnetic field can be modelled as a plane wave:

$$\underline{E} = E \cdot \hat{e} = \underline{E_o}(e^{i(kx-\omega t+\phi)} + c.c.) \tag{41}$$

"c.c." indicates the complex conjugate of the expression inside brackets.

The interaction term reads (assuming $\hat{d}$ and $\underline{E}$ points along the same direction),

$$\hat{H}^{(i)} = -\underline{\hat{d}} \cdot \underline{E}(t) = -\hat{d} \cdot E(t) \tag{42}$$

In this case, $\hat{d}$ is defined as the transition dipole moment operator. It provides the electric dipole moment associated with two different states. Thus, for two arbitrary states $|i\rangle \neq |f\rangle$:

$$\langle i|\,\hat{d}\,|f\rangle = \langle f|\,\hat{d}\,|i\rangle = d \tag{43}$$

$$\langle i|\,\hat{d}\,|i\rangle = \langle f|\,\hat{d}\,|f\rangle = 0 \tag{44}$$

Expanding Eq. (42) throughout a two-level system:

$$\hat{H}^{(i)} = (|g\rangle\langle e| + |e\rangle\langle g|)\langle i|\hat{H}^{(i)}|f\rangle = \frac{1}{2}\hbar\Omega(|g\rangle\langle e| + |e\rangle\langle g|) \times (e^{i(kx-\omega t)} + c.c.), \quad (45)$$

rewriting the constant as $\frac{1}{2}\hbar\Omega$, where $\hbar\Omega = dE_0$. It is convenient to understand Eq. (45) in terms of Pauli matrices (Eq. (10)): $|e\rangle\langle g| \mapsto \sigma_+ = \frac{1}{2}(\sigma_x + i\sigma_y)$, $\quad |g\rangle\langle e| \mapsto \sigma_- = \frac{1}{2}(\sigma_x - i\sigma_y)$

$$\hat{H}^{(i)} = \frac{1}{2}\hbar\Omega(\sigma_+ + \sigma_-) \times (e^{i(kx-\omega t)} + e^{-i(kx-\omega t)}) \quad (46)$$

This expression introduces the concept of Rabi frequency, namely, coupling frequency in a two-level quantum system which generates oscillations between the ground and the excited state. It can be interpreted as if the system periodically absorbs photons of the electromagnetic field. Thus, it is excited and the electron promotes to the higher energy state. After a certain time, the photon is reemitted by the system and the cycle is repeated. If the frequency of the laser is the same as the level transition, Ω can be interpreted as a measure of the strength of the coupled field-ion.

$$\Omega_{i,f} = \frac{d_{i,f} \cdot E_0}{\hbar} \quad (47)$$

Besides the specified frequency, it is important to define and differentiate the following quantities,

- ν := trap frequency (of the levels of the harmonic oscillator associated).
- ω := effective light frequency of the laser.
- ω_o := transition frequency of the ion at rest.
- $\delta = \omega - \omega_o$:= detuning.

In any case, the interesting picture is how electromagnetic fields couple with the ions. It will be studied in the interaction picture.

The interaction picture is an hybrid representation between the Schrödinger and Heisenberg picture. It is useful when one initially knows the exact solution for a part of the Hamiltonian, $\hat{H}_o$. In this way,

$$\hat{H}_o = \hat{H}^{(m)} + \hat{H}^{(e)} \quad (48)$$

and the time evolution propagator,

$$\hat{U}_0 = e^{-\frac{i}{\hbar}\hat{H}_o t}, \quad (49)$$

The interaction Hamiltonian in the interaction picture is:

$$\begin{aligned}\hat{H}_{\text{int}} &= \hat{U}_0^\dagger \hat{H}^{(i)} \hat{U}_0 = \\ &= \frac{1}{2}\hbar\Omega e^{(i/\hbar)\hat{H}^{(e)}t}(\hat{\sigma}_+ + \hat{\sigma}_-)e^{-(i/\hbar)\hat{H}^{(e)}t} \times e^{(i/\hbar)\hat{H}^{(m)}t}(e^{i(kx-\omega t+\phi)} + c.c.)e^{-(i/\hbar)\hat{H}^{(m)}t}.\end{aligned} \quad (50)$$

The two terms differentiated in Eq. (50) are expressed in the interaction picture. However, they evolve in a formal mode equivalent to Heisenberg picture but with a reduced Hamiltonian. Consequently, they obey observable Heisenberg's equation in Eq. (24).

Analyzing $\hat{\sigma}_+$ and $\hat{a}$ will be useful for future mathematical developments in this section.

$$\dot{\hat{\sigma}}_+ = \frac{i}{\hbar}[\hat{H}^{(e)}, \hat{\sigma}_+] = i\frac{\omega_o}{2}[\hat{\sigma}_z, \hat{\sigma}_+] = i\omega_o\hat{\sigma}_+ \tag{51}$$

$$\dot{\hat{a}} = \frac{i}{\hbar}[\hat{H}^{(m)}, \hat{a}] \simeq i\nu[\hat{a}^\dagger\hat{a}, \hat{a}] = -i\nu\hat{a} \tag{52}$$

Solving Eqs. (51) and (52):

$$\hat{\sigma}_+(t) = \hat{\sigma}_+ e^{i\omega_o t} \tag{53}$$

$$\hat{a}(t) = \hat{a}e^{-i\nu t} \tag{54}$$

In Eq. (52), as it has been established before, the movement of the ions inside a rf trap is modelled as an harmonic oscillator. Thus, this expression can be used correctly. At this point, Eq. (50) is,

$$\hat{H}_{\text{int}} = \frac{1}{2}\hbar\Omega\left(\hat{\sigma}_+ e^{i\omega_o t} + \hat{\sigma}_- e^{-i\omega_o t}\right) \times e^{(i/\hbar)\hat{H}^{(m)}t}(e^{i(kx-\omega t+\phi)} + c.c.)e^{-(i/\hbar)\hat{H}^{(m)}t}. \tag{55}$$

Attending to the second part of the expression, only the space dependent part of the plane waves will interact with $\hat{H}^{(m)}$. Likewise in Eq. (31), the spatial part can be decomposed in terms of ladder operators of a harmonic oscillator:

$$\hat{x} = \sqrt{\frac{2\hbar}{m\nu}}(\hat{a} + \hat{a}^\dagger) \tag{56}$$

This leads to,

$$k\hat{x} = \sqrt{\frac{\hbar}{2m\nu}}(\hat{a} + \hat{a}^\dagger) = \eta(\hat{a} + \hat{a}^\dagger), \tag{57}$$

We define the Lamb-Dicke parameter as,

$$\eta = kx_o = k\sqrt{\frac{\hbar}{2m\nu}}. \tag{58}$$

Afterwards, we consider the Heisenberg evolution of the operators in Eq. (57).

$$k\hat{x}_H(t) = \eta(\hat{a}(t) + \hat{a}^\dagger(t)) = \eta(\hat{a}e^{-i\nu t} + \hat{a}^\dagger e^{i\nu t}) \tag{59}$$

In addition, in the Hamiltonian two kinds of time dependent oscillatory terms appear, some with $\omega_o - \omega = \delta$ and the others with $\omega_o + \omega$. The latter can be neglected since they

oscillate much faster than the system time evolution. As a consequence, they do not disrupt the evolution of the ions. This is called a *Rotating wave approximation (RWA)* and the resulting Hamiltonian is (taking advantage of $(\hat{\sigma}_-)^\dagger = \hat{\sigma}_+$):

$$\hat{H}_{\text{int}}(t) = \frac{1}{2}\hbar\Omega_0\sigma_+ \exp\left\{i\eta\left(\hat{a}e^{-i\nu t} + \hat{a}^\dagger e^{i\nu t}\right)\right\} e^{i(\phi-\delta t)} + \text{H.c.} \tag{60}$$

"H.c." indicates the Hermitian conjugate of the expression.

This expression can be simplified if the ion is in the Lamb-Dicke regime. This means that the coupling induced by the external field between motional states and ion internal states is small enough such that

$$\sqrt{\langle(k\hat{x})^2\rangle} = \sqrt{\eta^2\langle(\hat{a}+\hat{a}^\dagger)^2\rangle} << 1 \tag{61}$$

When Lamb-Dicke regime is achieved, the recoil energy of the laser is negligible compared to the spacing energy of the harmonic oscillator levels and transitions changing the motional state of the ion are decoupled of ion internal transitions. Expanding Eq. (60) in power series of $\eta \ll 1$:

$$\hat{H}_{\text{QC}}(t) = \frac{1}{2}\hbar\Omega_0\sigma_+ \left\{1 + i\eta\left(\hat{a}e^{-i\nu t} + \hat{a}^\dagger e^{i\nu t}\right)\right\} e^{i(\phi-\delta t)} + \text{H.c.} \tag{62}$$

Equation (62) is also known as the basic Hamiltonian of an ion trap quantum computer. It will contain three resonances depending on the detuning, δ. When the system is in one of the resonances, the contributions of the other are not relevant (second RWA) and time dependent terms are negligible.

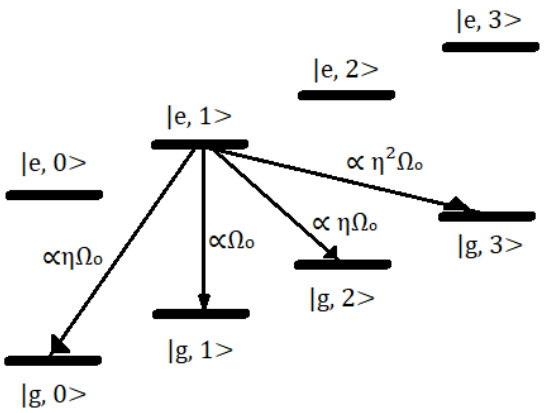

Figure 6: Relative strength of transitions in the Lamb-Dicke regime. The probability of having a transition involving more than one phonon decreases as η increases.

- Carrier resonance, $\delta = 0$. Transition of the type: $|n\rangle|g\rangle \leftrightarrow |n\rangle|e\rangle$. It has the form:

$$\hat{H}_{\text{car}} = \frac{1}{2}\hbar\Omega_0\left(\sigma_+ e^{i\phi} + \sigma_- e^{-i\phi}\right) \tag{63}$$

- First red sideband *(rsb)*, $\delta = -\nu$. Transition of the type: $|n\rangle|g\rangle \leftrightarrow |n-1\rangle|e\rangle$. In this interaction, while the ion promotes to the excited state, it absorbs a phonon (motion quantum). The form of the Hamiltonian is:

$$\hat{H}_{\text{rsb}} = \frac{i}{2}\eta\hbar\Omega_0\left(\sigma_+\hat{a}e^{i\phi} + \sigma_-\hat{a}^\dagger e^{-i\phi}\right) \tag{64}$$

  with Rabi frequency:

$$\Omega_{n,n-1} = \eta\Omega_0\sqrt{n} \tag{65}$$

- First blue sideband *(bsb)*, $\delta = +\nu$. Transition of the type: $|n\rangle|g\rangle \leftrightarrow |n+1\rangle|e\rangle$. It is the counterpart of *rsb* resonance. It adds a phonon while the ion promotes. Its form is:

$$\hat{H}_{\text{bsb}} = \frac{i}{2}\eta\hbar\Omega_0\left(\sigma_+\hat{a}^\dagger e^{i\phi} + \sigma_-\hat{a}e^{-i\phi}\right) \tag{66}$$

  with Rabi frequency:

$$\Omega_{n,n+1} = \eta\Omega_0\sqrt{n+1} \tag{67}$$

When η increases while standing in the Lamb-Dicke regime, transitions among more than one phonon are allowed but are less probable than first order resonances. It is necessary to expand Eq. (62) in a power series to higher order in η.

3.4 Ion cooling

In order to start a quantum computing, it is necessary to know the initial state of the system to make correct predictions of its behaviour.

This can be achieved via cooling the ions of the rf trap to the ground state of the trapping potential. Besides, this process sets the system in the Lamb-Dicke regime. Thus, the Hamiltonian approximations in Eq. (61) are valid.

$$k_{\text{B}}T \ll \hbar\nu \tag{68}$$

Ion cooling is commonly realized as a two-step procedure. First stage is called Doppler cooling which can reduce the temperature of ions to a certain limit. After reaching this temperature, a second stage cooling is required for ground state guarantees. There exist different methods to reach it but, as a brief introduction, we will discuss *EIT cooling* (electromagnetically induced transparency).

3.4.1 Doppler cooling

A complete treatment requires a rigorous analysis which is far beyond this study. Instead, we will analyse a simple model where micromotion from secular motion is neglected. This effect was studied in global picture by Cirac, Galay *et al.* **[9]**.

Considering Eq. (21), when micromotion is omitted, it can be approximated as a time-independent harmonic oscillator potential:

$$V_{\mathrm{rf}}(x) \approx \frac{1}{2} m v^2 x^2 \tag{69}$$

Taking a classical description of the trapped ion movement inside the potential, its velocity will be,

$$v(t) = v_0 \cos(\nu t) \tag{70}$$

The laser radiation pressure is described as a continuous force when radiative decay time, Γ (the average time an ion emits) is much shorter than an ion oscillation: $\Gamma \gg \nu$. In one absorption-emission cycle, the ion velocity remains constant.

Along one direction, the ion momentum will raise $\Delta p = \hbar k$ each time it absorbs a photon. Emission will be in every direction. Eventually, it will lead to a zero-momentum average transfer and a *Brownian motion* in momentum space.

The probability of being in the excited state is given through Bloch equations **[10]**.

$$\rho_{ee} = \langle e | \, \hat{\rho} \, | e \rangle = \frac{s/2}{1 + s + (2\delta_{\mathrm{eff}}/\Gamma)^2} \tag{71}$$

Defining s as the saturation parameter,

$$s = 2|\Omega|^2/\Gamma^2 \tag{72}$$

For $s \gg 1 \rightarrow \rho_{ee} \approx 1/2$ and the system is in a superposition of ground and excited state. Otherwise, if $s \ll 1$, the whole system is almost in the ground state.

Another parameter we consider is the global detuning composed by the Doppler shift and the laser detuning,

$$\delta_{\mathrm{eff}} = \delta - \underline{k} \cdot \underline{d}. \tag{73}$$

Consequently, the average force on the ions in the model is,

$$\left(\frac{dp}{dt} \right)_a \approx \langle F_a \rangle = \hbar k \Gamma \rho_{ee}. \tag{74}$$

This absortion force can be linearized employing a Taylor series $(1+x^2)^{-1} \sim 1-x^2+\ldots$, if v is enough small (it implies $\delta_{\text{eff}} \ll \Gamma$).

$$F_a \approx F_0(1+\kappa v), \qquad F_0 = \hbar k \Gamma \frac{s/2}{1+s+(2\delta/\Gamma)^2} \tag{75}$$

and κ is the friction coefficient.

$$\kappa = \frac{8k\delta/\Gamma^2}{1+s+(2\delta/\Gamma)^2} \tag{76}$$

It will define the nature of the force depending on the detuning sign. If $\delta > 0$, it will contribute to increase the kickback. On the other hand, when $\delta < 0$, the force will present a damping proportional to v.

The cooling evolution of the system will be equivalent to the energy dissipated by the system and the kinetic term time evolution:

$$\dot{E}_c = \langle F_a v \rangle = F_0 \left(\langle v \rangle + \kappa \left\langle v^2 \right\rangle \right) \tag{77}$$

Evaluating Eq. (70), $\langle v \rangle = 0$ and:

$$\dot{E}_c = F_0 \kappa \langle v^2 \rangle < 0 \tag{78}$$

Nevertheless, $\rho_{\text{ee}}(v=0) \neq 0$. Even if the ion is at rest, it will continue absorbing-emitting photons (near steady state). At this point, both processes will have the same rate but different directions. Experimentally, it has been tested that the emission recoil kick over the ion motion axis is $\xi = 2/5$ for dipole radiation. **[11]**.

The heating rate will be,

$$\dot{E}_h = \frac{1}{2m}\frac{d}{dt}\left\langle p^2 \right\rangle = \dot{E}_{\text{abs}} + \dot{E}_{\text{em}} = E_{\text{abs}}(1+\xi) \simeq \frac{1}{2m}(\hbar k)^2 \Gamma \rho_{ee}(v=0)(1+\xi), \tag{79}$$

considering that $\langle p \rangle = 0$. We also neglect emission and absorption correlation.

If the ion is in equilibrium, Eq. (78) must be equal to Eq. (79), such that,

$$F_0 \kappa \langle v^2 \rangle = \frac{1}{2m}(\hbar k)^2 \Gamma \rho_{ee}(v=0)(1+\xi). \tag{80}$$

One can assume the thermal energy will be of the order of kinetic energy.

$$U_T = k_B T \sim E = m\langle v^2 \rangle \tag{81}$$

Rearranging Eq. (80) and expanding F_0, κ and $\rho_{ee}(v=0)$:

$$k_B T \approx m\left\langle v^2\right\rangle = \frac{\hbar\Gamma}{8}(1+\xi)\left[(1+s)\frac{\Gamma}{2\delta}+\frac{2\delta}{\Gamma}\right] \tag{82}$$

Even for this simple model, in which many cooling trap effects are neglected, there exists a minimal temperature,

$$T_{\min} = \frac{\hbar\Gamma\sqrt{1+s}}{4k_B}(1+\xi), \tag{83}$$

for a detuning

$$\delta = \frac{1}{2}\Gamma\sqrt{1+s}, \tag{84}$$

obtained minimizing $T(\delta)$ in Eq. (82).

In conclusion, the ion will lose energy if cooling events are more likely than heating events. The limit is reached when both processes are equally likely.

3.4.2 EIT cooling

The main purpose of the electromagnetic induced transparency (EIT) cooling is to set the initial state of the ion trap in the ground state $|0\ldots0\rangle$.

We consider a three-level system with two lasers coupling ground and an auxiliary state with the excited state applying a detuning. Both lasers have different strengths. Precooling the ions to the Lamb-Dicke regime forbids transitions with $\Delta n > 1$.

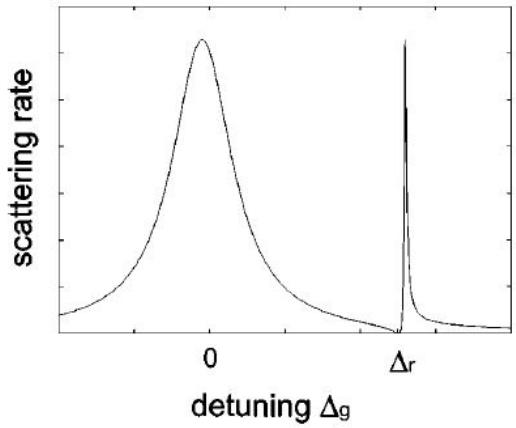

Figure 7: Scattering rate of the transitions as a function of the weak laser detuning. Source in Ref. **[12]**.

The idea of this method relies in the fact that, when $\delta_g \approx \delta_r$, a resonance effect appears which suppresses the carrier scattering. The strong laser (δ_r) links $|e\rangle \leftrightarrow |r\rangle$ and it pumps ions to $|g\rangle$. The weak laser interferes and the transition $|e\rangle \leftrightarrow |g\rangle$ is less probable.

Finally, the system will be found in its ground state. A necessary condition to be certain is to choose $\delta_g \approx \delta_r \gg \Gamma$.

4 Trapped-ion quantum computing

In this chapter, I will discuss how the ions in rf traps can be manipulated via laser pulses to perform quantum gates,

We will first review quantum-state preparation. It has been assumed for this analysis that system levels are stable (they have an infinite lifetime), which is only fulfilled if residual interactions are neglected. This approximation can be done properly because the time scale for quantum gates is significantly smaller than the state lifetime.

The most general state will take the form:

$$|\Psi(t)\rangle = \sum_{n=0}^{\infty} c_{n,g}(t)\,|n,g\rangle + c_{n,e}(t)\,|n,e\rangle \tag{85}$$

Choosing a large detuning one obtains:

$$\delta = l\nu + \delta' \;\; (\; \delta' \ll \nu,\; l \in \mathbb{Z}) \tag{86}$$

The state will be resonant with the l-th blue sideband. Thus, with the general Hamiltonian in Eq. (60), only the l-th term of the Taylor expansion ($\eta \ll 1$) is going to interact.

$$\exp\left\{i\eta\left(\hat{a}^\dagger e^{i\nu t}\right)\right\} \approx 1 + i\eta\hat{a}^\dagger e^{i\nu t} + \frac{(i\eta)^2}{2!}(\hat{a}^\dagger)^2 e^{i2\nu t} + \ldots \quad \overbrace{\longrightarrow}^{l-th\ term} \quad \frac{(i\eta)^l}{l!}(\hat{a}^\dagger)^l e^{il\nu t}, \tag{87}$$

and analogously to the $\hat{a}$ term.

The time evolution is governed by the Schrödinger equation,

$$i\hbar\frac{d\,|\Psi(t)\rangle}{dt} = \hat{H}_{\rm int}\,|\Psi(t)\rangle\,. \tag{88}$$

Developing the fist side of Eq. (88), since eigenstates of $|\Psi(t)\rangle$ are time-independent we achieve

$$i\hbar\frac{d\,|\Psi(t)\rangle}{dt} = i\hbar\left(\sum_{n=0}^{\infty}\dot{c}_{n,g}(t)\,|n,g\rangle + \dot{c}_{n,e}(t)\,|n,e\rangle\right). \tag{89}$$

On the other side, we have the four terms that, in principle, are resonant in the interaction Hamiltonian,

$$\hat{H}^r_{\rm int} = \frac{\hbar}{2}\Omega_0(\frac{(i\eta)^l}{l!})\{\sigma_+\left((\hat{a})^l e^{-il\nu t} + (\hat{a}^\dagger)^l e^{il\nu t}\right)e^{i(\phi-\delta' t)} + \text{H.c.}\}. \tag{90}$$

Nevertheless, the action over $|n,g\rangle$ and $|n,e\rangle$ are not zero only in the cases,

$$\sigma_+(\hat{a}^\dagger)^l\,|n,g\rangle = \sqrt{(n+l)!}\,|n+l,e\rangle \tag{91}$$

$$\sigma_-(\hat{a})^l\,|n+l,e\rangle = \sqrt{(n+l)!}\,|n,g\rangle\,, \qquad n>l \tag{92}$$

With the aim to rewrite Eq. (88) as a set of equations for the $c_{i,j}$ coefficients, it will be projected over arbitrary states $\langle n,g|$ and $\langle n+l,e|$ respectively.

Case $\langle n,g|\cdot$ [Eq. (88)]:

$$i\hbar\,\langle n,g|\,\frac{d}{dt}\,|\Psi(t)\rangle = \langle n,g|\,\hat{H}^r_{\rm int}\,|\Psi(t)\rangle \tag{93}$$

Analyzing term by term:

$$\langle n,g|\cdot i\hbar\frac{d\,|\Psi(t)\rangle}{dt} = ih\dot{c}_{n,g}(t)\,\langle n,g|n,g\rangle = ih\dot{c}_{n,g}(t), \tag{94}$$

because $\langle n,g|m,g\rangle = \delta_{nm}$.

The interaction matrix element is,

$$\langle n,g|\,\hat{H}^r_{\rm int}\,|\Psi(t)\rangle = \frac{\hbar}{2}\Omega_0(\frac{(i\eta)^l}{l!})\,\langle n,g|\,\sigma_+(\hat{a}^\dagger)^l e^{il\nu t}e^{i(\phi-\delta t)} + \sigma_-\hat{a}^l e^{-il\nu t}e^{-i(\phi-\delta t)})\,|\Psi(t)\rangle \tag{95}$$

which is not zero for the term $c_{n+l,e}(t)$, applying Eq. (92),

$$\langle n,g|\,\hat{H}^r_{\rm int}\,|\Psi(t)\rangle = \frac{i^l\hbar}{2}\Omega_0\frac{\eta^l}{l!}\sqrt{(n+l)!}e^{-il\nu t}e^{-i(\phi-\delta t)}c_{n+l,e}(t). \tag{96}$$

In this case, the form of δ [Eq. (86)] cancels the evolution part of $\hat{a}$ operator: $-il\nu t - i(\phi-\delta t) = -il(\phi-\delta' t)$ and the generalized Rabi frequency for an l-number state jump is $\Omega_{n+l,n} = \Omega_0\eta^l\sqrt{(n+l)!}/l!$.

The final expression is

$$\langle n,g|\,\hat{H}^r_{\rm int}\,|\Psi(t)\rangle = i^l\frac{\hbar}{2}\Omega_{n+l,n}e^{-i(\phi-\delta' t)}c_{n+l,e}(t) \tag{97}$$

Matching both sides, Eq. (94) and Eq. (97), we obtain the following expression,

$$\dot{c}_{n,g}(t) = -i^{(1-|l|)}e^{i(\delta' t-\phi)}\frac{\Omega_{n+l,n}}{2}c_{n+l,e}(t). \tag{98}$$

The second coupled equation can be deduced similarly but projecting Eq. (88) over $|n+l,e\rangle$, in which it is necessary to use Eq. (91).

$$\dot{c}_{n+l,e}(t) = -i^{(1+|l|)} e^{-i(\delta' t-\phi)} \frac{\Omega_{n+l,n}}{2} c_{n,g}(t). \tag{99}$$

The system of coupled equations can be solved using Laplace transform method. The following properties of the transform will be used.

1. Laplace transform of a function derivative.

$$\mathcal{L}[f'(t)] = s\mathcal{L}[f(t)] - f(0). \tag{100}$$

2. Laplace transform of an exponential multiplying a function.

$$\mathcal{L}[e^{-at} f(t)] = F(s+a). \tag{101}$$

3. Inverse transform of a dumped sine or cosine.

$$\mathcal{L}^{-1}\left[\frac{b}{(s+a)^2+b^2}\right] = e^{-at}(bt), \qquad \mathcal{L}^{-1}\left[\frac{s+a}{(s+a)^2+b^2}\right] = e^{-at}\cos(bt), \tag{102}$$

where s is a complex variable and $a, b \in \mathbb{R}$. To simplify notation, in Eq. (98), Eq. (99), the time-independent terms will be written as:

$$K \equiv i^{1-|l|} e^{-i\phi} \Omega_{n+l,n}/2 \qquad \widetilde{K} \equiv i^{1+|l|} e^{-i\phi} \Omega_{n+l,n}/2$$

being $K\widetilde{K} = -\Omega^2_{n+l,n}/4$. The transformed functions will be denoted by $\mathcal{L}[c_{n,g}(t)] \equiv G(s)$, $\mathcal{L}[c_{n+l,e}(t)] \equiv E(s)$. After applying Eqs. (100) and (101), the transformed coupled equations are:

$$\begin{cases} sG(s) - c_{n,g}(0) = -KE(s-i\delta) \\ sE(s) - c_{n+l,e}(0) = -\widetilde{K}G(s+i\delta) \end{cases} \tag{103}$$

After some algebra, it can be written as a function of the initial conditions. The following analysis is restricted to calculate $c_{n,g}(t)$. This process is analogue to $c_{n+l,e}(t)$.

$$G(s) = \frac{s-i\delta}{s(s-i\delta)+\Omega^2_{n+l,n}/4} c_{n,g}(0) - \frac{K}{s(s-i\delta)+\Omega^2_{n+l,n}/4} c_{n+l,e}(0) \tag{104}$$

Finally, the transformation must be inverted to recover the solution. The inverse Laplace transform has no effect over constant values. Thus, its action in Eq. (104) will be equivalent to solving a dumped sine or cosine [Eq. (102)].

The final solution is,

$$\begin{pmatrix} c_{n+l,e}(t) \\ c_{n,g}(t) \end{pmatrix} = T_n^l \begin{pmatrix} c_{n+l,e}(0) \\ c_{n,g}(0) \end{pmatrix}, \tag{105}$$

with

$$T_n^l = \begin{pmatrix} e^{-i(\delta'/2)t}\left[\cos\left(f_n^l t/2\right) + i\frac{\delta'}{f_n^l}\sin\left(f_n^l t/2\right)\right] & -i\frac{\Omega_{n+l,n}}{f_n^l}e^{i(\phi+|l|\pi/2-\delta' t/2)}\sin\left(f_n^l t/2\right) \\ -i\frac{\Omega_{n+l,n}}{f_n^l}e^{-i(\phi+|l|\pi/2-\delta' t/2)}\sin\left(f_n^l t/2\right) & e^{i(\delta'/2)t}\left[\cos\left(f_n^l t/2\right) - i\frac{\delta'}{f_n^l}\sin\left(f_n^l t/2\right)\right] \end{pmatrix}, \tag{106}$$

and $f_n^l = \sqrt{\delta'^2 + \Omega_{n+l,n}^2}$.

This is a generalized solution of the behaviour of a two-level quantum system and a laser resonant for the l-th sideband. It describes a Rabi floppling between ground and excited state.

4.1 Single-qubit gates with carriers

The starting point of most ion gates is the ground state of motion. Besides, to reach this ground state the system must be inside the Lamb-Dicke regime.

In a single trap, it is difficult to implement multi and single-qubit gates due to the fact that it requires a strong laser manipulation. At ion-ion distance, laser beams must be extremely narrow. A solution could be to address the ions in a perpendicular direction to the trap axis. Nevertheless, it will strongly decrease the laser-axial motion coupling. Currently, one of the most appropriate methods is to split single pulses into composite pulses.

In this section, we will discuss only the creation of single qubit gates.

4.1.1 Creation of number states

At the first place, the ion is precooled to $|\Psi(0)\rangle = |g, n = 0\rangle$. The objective will be to modify the number state applying multiple π-*pulses*. A π-*pulse* will take a resonance frequency of the trap, thus in Eq. (86), $\delta' = 0$. It must fulfill the condition

$$f_n^l t_{\pi,n} = |\Omega_{n+l,n}|\, t_{\pi,n} = \pi \tag{107}$$

where $t_{\pi,n}$ is the time pulse.

With this requirement, Eq. (106) simplifies for the carrier and the sidebands to:

$$T_n^0 = \begin{pmatrix} 0 & -ie^{i\phi} \\ -ie^{-i\phi} & 0 \end{pmatrix} \qquad T_n^{\pm 1} = \begin{pmatrix} 0 & e^{i\phi} \\ -e^{-i\phi} & 0 \end{pmatrix} \tag{108}$$

disregarding the global phase (not measurable). If the state is a superposition of number states, the relative phase is relevant.

The technique to raise the number state is to create a ladder of blue and red sideband pulses. The ion may follow the next level scheme:

$$|0,g\rangle \longrightarrow T_0^1 |0,g\rangle = |1,e\rangle \longrightarrow T_1^{-1} |1,e\rangle = |2,g\rangle \longrightarrow \dots \tag{109}$$

Finally, if the final state of the qubit is excited one can apply a carrier pulse to produce $|m,g\rangle$ state.

$$|m,e\rangle \longrightarrow T_1^0 |m,e\rangle = -i |m,g\rangle , \quad m \in \mathbb{N} \tag{110}$$

in a single-qubit operation, the global phase will not take any real effect.

A motional state can be detected due to the fact that Rabi frequency is different for each state [Eqs. (65) and (67)]. Inside Lamb-Dicke regime, the most important transitions are the first blue and red sidebands (outside this regime frequency behaviour is more complicated to distinguish).

Measuring the probability of finding the ion in the ground state after a blue sideband pulse ($l = +1$) one will obtain

$$P_g(t) = \left\langle \Psi(t) \left| \left(|g\rangle\langle g| \otimes \hat{I}_m \right) \right| \Psi(t) \right\rangle . \tag{111}$$

In this case, $|\Psi(t)\rangle$ corresponds to a general state [Eq. (85)] projected on any motional state in the ground state. $\hat{I}_m$ is the identity operator of the motional space.

Therefore, Eq. (106) will have the form ($\delta' = 0$):

$$T_n^{+1} = \begin{pmatrix} \cos\left(\frac{1}{2}\Omega_{n,n+1}t\right) & 0 \\ 0 & \cos\left(\frac{1}{2}\Omega_{n,n+1}t\right) \end{pmatrix} \tag{112}$$

Furthermore, utilizing the equality $\cos^2(a) = \frac{1+\cos(2a)}{2}$ and the probability normalization $\sum_n^| c_n(0)|^2 = 1$

$$P_g(t) = \sum_{n=0}^{\infty} |c_n(t)|^2 = \frac{1}{2}\left[1 + \sum_{n=0}^{\infty} |c_n(0)|^2 \cos\left(\Omega_{n,n+1}t\right)\right] \tag{113}$$

Consequently, the population of each state $P_n = |c_n(0)|^2$ is deduced by Fourier transforming Eq. (113):

$$\mathcal{F}\{P_g(t)\} = \sqrt{\frac{\pi}{2}}\left\{\delta(\omega) + \frac{1}{2}\sum_{n=0}^{\infty} P_n \left[\delta(\omega - \Omega_{n+1,n}) + \delta(\omega + \Omega_{n+1,n})\right]\right\} \tag{114}$$

where $\delta(\omega \pm a)$ is the Dirac delta function.

Experimentally, in Eq. (111) the signal is damped for each n. Thus, to fit the data, we have introduced n-dependent exponential functions with a constant modelled as: $\gamma_n \approx \gamma_0(n+1)^{0,7}$.

$$P_g(t) = \frac{1}{2}\left[1 + \sum_{n=0}^{\infty} P_n \cos\left(\Omega_{n,n+1}t\right) e^{-\gamma_n t}\right] \tag{115}$$

Some explanations to this phenomenon associate dumping to intensity fluctuations of lasers and magnetic fluctuations at the ion position.

4.1.2 Creation of coherent states

A coherent state $|\alpha\rangle$ of the ion is defined as a state that minimizes the wave packet uncertainty in the position representation. They are Gaussian-shaped and oscillate classically in a harmonic well. A way to define coherent states is as the action of the displacement operator on the vacuum:

$$\hat{D}(\alpha) = \exp\left[\alpha\hat{a}^{\dagger}(t) - \alpha^{*}\hat{a}(t)\right], \quad \alpha \in \mathbb{C} \tag{116}$$

and

$$|\alpha\rangle = \hat{D}(\alpha)\,|0\rangle \tag{117}$$

Physically, the displacement operator can be interpreted as a phase shift in optical phase space. It has a group structure and the action of this operator on a coherent state is

$$|\Psi'\rangle = \hat{D}(\alpha)\,|\Psi\rangle \tag{118}$$

There are different paths to achieve coherent states, including pairs of stationary waves, a spatially uniform driving field, inter alia.

The second method will be discussed hereinafter. The homogeneous field is described as a force of the form:

$$F(t) = eE_0(\omega_d t - \varphi) \tag{119}$$

in which ω_d is the drive frequency.

In a homogeneous force, if the position operator is reexpressed in terms of Eq. (32), the interaction term will be

$$H_I = -F(t)\hat{x} = -eE_0(\omega_d t - \varphi)\sqrt{\frac{\hbar}{2m\nu}}\left\{\hat{a}u^{*}(t) + \hat{a}^{\dagger}u(t)\right\} \tag{120}$$

It is enough to consider a first-order approximation to analyze the resonant behaviour of the system. In this case, when we neglect in Eq. (29) the sum for $n \geq \pm 2$ and $\nu = \beta_x\omega_{rt}/2.$,

$$u(t) \approx e^{i\nu t}\left\{\left[1 + \left(\frac{q_x}{2}\right)\cos\left(\omega_{\mathrm{rf}}t\right)\right] / \left(1 + \frac{q_x}{2}\right)\right\}. \tag{121}$$

The laser will only interact if the drive is resonant with the ion motion. Choosing $\omega_d = \nu$ and expanding the sine using *Euler relationships*, we obtain

$$H_I = -eE_0\sqrt{\frac{\hbar}{2m\nu}}\frac{e^{i(\nu t-\varphi)} - e^{-i(\nu t-\varphi)}}{2i}\left(\hat{a}e^{-i\nu t} + \hat{a}^\dagger e^{i\nu t}\right)\frac{\left[1 + \left(\frac{q_x}{2}\right)\cos\left(\omega_{\mathrm{r}} t\right)\right]}{\left(1 + \frac{q_x}{2}\right)}. \tag{122}$$

In this equation, the rotating term with frequency 2ν can be neglected (RWA). Likewise, non-steady terms can be discarded. The approximate interaction Hamiltonian is,

$$H_I \approx \frac{-eE_0}{2i}\frac{1}{1+\frac{q_x}{2}}\sqrt{\frac{\hbar}{2m\nu}}\left(\hat{a}e^{-i\varphi} + \hat{a}^\dagger e^{i\varphi}\right) \tag{123}$$

The evolution of the system is governed by the time evolution operator [Eq. (49)] with the interaction Hamiltonian [Eq. (120)]. Introducing Eq. (123), it takes the form of a displacement operator [Eq. (116)]

$$U(t) = \exp\left[\left(\Omega_d t\right)\hat{a}^\dagger - \left(\Omega_d^* t\right)\hat{a}\right] = D\left(\Omega_d t\right) \tag{124}$$

with

$$\alpha = \Omega_d \cdot t = \frac{-eE_0}{2\hbar}\frac{1}{1+\frac{q_x}{2}}\sqrt{\frac{\hbar}{2m\nu}}e^{i\varphi}\cdot t \tag{125}$$

Thus, the time the drive is operating is proportional to the coherent displacement.

4.1.3 Creation of squeezed states

A squeezed state is a non-classical state of the system for which the position or momentum variance is lower than the position and momentum variance of the ground state (which are equivalent to coherent states because they are minimum-uncertainty states too).

The variance of an operator will be denoted as: $\Delta Y = \sqrt{\langle Y^2\rangle - \langle Y\rangle^2}$

Any quantum system must fulfill Heisenberg uncertainly relations hence, if the position variance is squeezed, the momentum variance will become wider.

Squeezed states can be defined as the action of the squeeze operator in vacuum,

$$S(\zeta) = \exp\left[\frac{1}{2}\left(\zeta^*\hat{a}^2 - \zeta\hat{a}^{\dagger 2}\right)\right], \qquad \zeta \in \mathbb{C} \tag{126}$$

being $\hat{a}, \hat{a}^\dagger$ ladder operators.

It can be interpreted as a two-photon generalization of the displacement operator [Eq. (116)]. As ladder operator appears in pairs, only even-n levels will be populated.

For this type of states, we define the parameter β_s which gives information of the squeezing of the state,

$$\beta_s = \frac{\Delta x_0}{\Delta x_s}. \tag{127}$$

Δx_0 represents the variance of the ground state. If $\beta_s > 1$, the position dispersion is tighter than the ground state one. Otherwise, when $0 < \beta_s < 1$, the momentum variance is narrower.

Those states could be created from three sources: by a change in the rf trap spring constant, as a combination of steady/traveling wave lasers and by a parametric drive at 2ν.

The last method is similar to the one employed for creating coherent states. In this case, a 2ν frequency is necessary as a consequence of the odd-n levels being depopulated. β_s grows with the driving laser time in an exponential way. Thus, for short time periods an important percentage of the population is in high-n states ($n > 20$). As soon as n increases, the difference between Rabi frequencies decreases [Eq. (67)] and it is harder to distinguish frequencies. This is an important error source.

4.1.4 Schrödinger-cat states of motion

In the field of quantum optics, a "Schrödinger-cat" state refers to a linear combination of two motional coherent states $|\alpha\rangle$ and $|\alpha'\rangle$ where its wave-packet width is smaller compared to its spatial separation to avoid decoherence.

For a single trapped ion, the analogous form is the superposition:

$$|\alpha, g\rangle + |\alpha e^{i\phi}, e\rangle \tag{128}$$

This state can be achieved by using a pair of Raman laser beams. The relative phase at any step can be controlled by phase locking. Excited internal states are not affected by displacement beams because they are polarized σ^+.

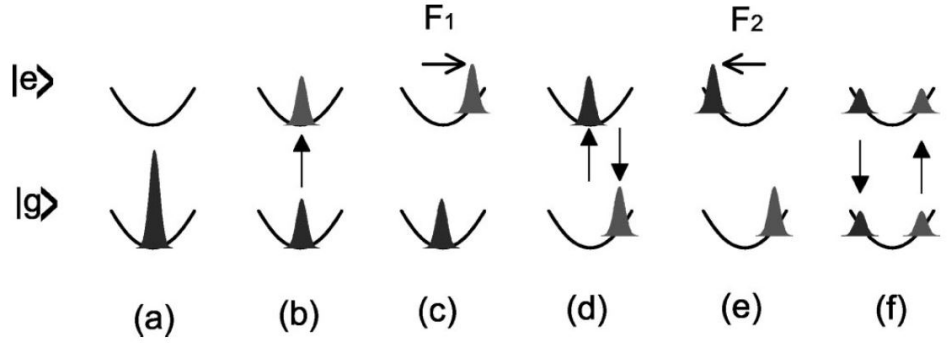

Figure 8: Steps of a Schrödinger-cat state creation. Source in Ref. **[13]**.

The explicit form of a $\pi/2$ and π pulse can be found from Eq. (106)

$$T_n^0(\frac{\pi}{2},\phi) = \frac{1}{\sqrt{2}}\begin{pmatrix} 1 & -ie^{i\phi} \\ -ie^{-i\phi} & 1 \end{pmatrix} \qquad T_n^0(\pi,\phi) = \begin{pmatrix} 0 & -ie^{i\phi} \\ -ie^{-i\phi} & 0 \end{pmatrix} \tag{129}$$

We will chose for Eq. (129): $\phi = -\pi/2$.

The process is summarized in the following sequence **[12]**,

(a) Precooling to ground state:

$$|\Psi_a\rangle = |n=0\rangle\,|g\rangle\,. \tag{130}$$

(b) Carrier $\pi/2$-pulse to split the state (relative phase remains constant)

$$|\Psi_b\rangle = T_n^0(\frac{\pi}{2},-\frac{\pi}{2})\,|0\rangle\,|g\rangle = \frac{1}{\sqrt{2}}\left(|0\rangle\,|g\rangle + |0\rangle\,|e\rangle\right). \tag{131}$$

(c) Displacement beam excites motion of $|e\rangle$

$$|\Psi_c\rangle = \hat{D}_e(\alpha)\,|\Psi_b\rangle = \frac{1}{\sqrt{2}}\left(|0\rangle\,|g\rangle + |\alpha\rangle\,|e\rangle\right), \tag{132}$$

where the sub-index e means that it only interacts with the excited state and $\hat{D}_e$ is the displacement operator.

(d) Carrier π-pulse to swap internal states:

$$|\Psi_d\rangle = T_n^0(\pi,-\frac{\pi}{2})\,|\Psi_c\rangle = \frac{1}{\sqrt{2}}\left(|\alpha\rangle\,|g\rangle + |0\rangle\,|e\rangle\right) \tag{133}$$

(e) Displacement beam of the second laser: $\hat{D}_e(\alpha e^{i\phi})$

$$|\Psi_e\rangle = \hat{D}_e(\alpha e^{i\phi})\,|\Psi_d\rangle = \frac{1}{\sqrt{2}}\left(|\alpha\rangle\,|g\rangle + \left|\alpha e^{i\phi'}\right\rangle|e\rangle\right) \tag{134}$$

the relative phase between coherent states is fixed to $\phi' = \pi$. Therefore,

$$|\Psi_e\rangle = \frac{1}{\sqrt{2}}\left(|\alpha\rangle\,|g\rangle + |-\alpha\rangle\,|e\rangle\right) \tag{135}$$

(f) Final $\pi/2$ pulse on the carrier (with $\phi = -\pi/2$) creates a superposition of both coherent states in each internal state:

$$|\Psi_f\rangle \approx \frac{1}{2}[|g\rangle(|-\alpha\rangle - |\alpha\rangle) + |e\rangle(|-\alpha\rangle + |\alpha\rangle)] \tag{136}$$

The accuracy of this method depends on the relative-phase lock. This results in destructive interference of the states. Schrödinger-cat states can be used to study quantum entanglement between ions **[14]**.

This procedure can be extended to generate arbitrary motional states on single-ion traps.

4.2 Mølmer-Sørensen gates

The Mølmer-Sørensen (MS) **[15]** gate is a two qubit gate to entangle two ions. It is created via pumping a bichromatic laser field tuned close to first blue and red sidebands.

Thereafter, we will briefly describe the procedure to deduce MS gate operator **[16]**, **[17]**.

The Hamiltonian of both lasers will have the form of Eq. (64) and Eq. (66) but with a detuning. The total Hamiltonian can be approximated to the sum of independent laser Hamiltonians.

$$H_{MS,n} \approx \frac{1}{2}\eta\hbar\Omega_{o,n}\left(\sigma_{+,n}e^{i\phi} + \sigma_{-,n}e^{-i\phi}\right)\left(ae^{i\delta t} + a^{\dagger}e^{-i\delta t}\right) \tag{137}$$

where rewriting $\sigma_{\pm}$ in terms of Pauli matrices the first part of the expression is:

$$\sigma_n = \left(\sigma_{+,n}e^{i\phi} + \sigma_{-,n}e^{-i\phi}\right) = \left(\sigma_{x,n}\cos\left(\phi\right) + \sigma_{y,n}\sin\left(\phi\right)\right), \tag{138}$$

The total spin contribution of the two ions interacting with MS gates will be,

$$S_{\phi} = \sum_{n=1}^{2}\sigma_n = \sum_{n=1}^{2}\left(\sigma_{x,n}\cos\left(\phi\right) + \sigma_{y,n}\sin\left(\phi\right)\right). \tag{139}$$

At this point, it is convenient to define Magnus expansion series in order to provide a path for calculating the time evolution operator. It is defined as an infinite sum of exponentials of the form,

$$U(t,0) = \exp\left\{\left(\frac{-i}{\hbar}\sum_{\kappa}\vartheta_{\kappa}(t)\right)\right\} \tag{140}$$

This expansion relies in the hypothesis that the solution can be written in this form. In this case, the relevant term is ϑ_2 as the first term will result as a displacement of the motional states and extra terms will vanish. The second-term expression is:

$$\vartheta_2(t) = \frac{1}{2}\int_0^t dt_1 \int_0^{t_1} dt_2 \left[H_I\left(t_1\right), H_I\left(t_2\right)\right] \tag{141}$$

with $\left[H_{MS}\left(t_1\right), H_{MS}\left(t_2\right)\right] = \frac{i}{2}(\eta\hbar\Omega_0 S_{\phi})^2[\delta(t_1 - t_2)]$

The final form of this expression can be found via including constants in θ parameter **[18]**. S_x, S_y are the sum of the x and y components of the spin of all ions respectively.

$$\mathcal{U}_{\mathrm{MS}}(\theta,\phi) = \exp\left[-i\theta\left(\cos\phi S_x + \sin\phi S_y\right)^2/4\right] \tag{142}$$

The action of this gate on the two-ion basis is:

$$\begin{aligned}
|ee\rangle &\to (|ee\rangle + \mathrm{i}|gg\rangle)/\sqrt{2} \\
|eg\rangle &\to (|eg\rangle + \mathrm{i}|ge\rangle)/\sqrt{2} \\
|ge\rangle &\to (|ge\rangle + \mathrm{i}|eg\rangle)/\sqrt{2} \\
|gg\rangle &\to (|gg\rangle + \mathrm{i}|ee\rangle)/\sqrt{2}
\end{aligned} \tag{143}$$

Therefore, it can be used to create entangled states **[19]**. The main problem of this kind of gate is, as other two-qubit gates, that its operation time is slower than single-qubit gates and than the trap frequency.

On the other hand, expressing the qubit states in the Hadamard basis,

$$|\pm\rangle = \frac{1}{\sqrt{2}}\left(|e\rangle \pm |g\rangle\right) \tag{144}$$

the action of MS operator on Eq. (143) can be seen as a $\pi/2$-delay of the phase θ, i.e., it is interpreted as a rotation of 90º degrees of the Bloch sphere.

$$\begin{aligned}
|++\rangle &\to |++\rangle \\
|+-\rangle &\to i|+-\rangle \\
|-+\rangle &\to i|-+\rangle \\
|--\rangle &\to |--\rangle
\end{aligned} \tag{145}$$

The MS gate establishes a method to experimentally identify if qubits 1 and 2 are in the same state. This idea can be exploited to employ it as a local CNOT gate. The set of one-qubit gates and MS gate constitutes a universal set of universal quantum gates **[20]**. In other words, any operation of a quantum computer can be expressed as a finite combination of these gates.

4.3 Tomography of quantum states

The creation of an arbitrary state in an ion trap is definitely important in order to manipulate information using qubits. Nevertheless, the action of measuring the qubit state is equally important. A state tomography on the ion states would record all the information available on

the system. Thus, it allows to analyze the data obtained without requiring subsequent measurements.

Over the course of trapped-ion Quantum Computing there have been many methods proposed to recover the motional states and recreate the full density matrix of the system. Let us highlight some of them. In 1995, Wallentowitz & Vogel **[21]** proposed to recover motional states via laser field pulses tuned at the same time at the first red and blue sideband. Other technique applied is the use of sidebands which combines micro and macromotion to check the state evolution of ions (1996, Bardroff *et al.* **[22]**). In the same year, Leibfried *et al.* **[23]** tried to employ coherent displacements on the blue sideband to recreate the density matrix. The technique was improved next year by Freyberger **[24]** adding a filter to measure the motional ground state population as well. Another interesting tomography process would be one which only measures a previously selected part of the ions which must leave the unmeasured ions states coherent. It was achieved using segmented ion traps in 2004 by Barrett *et al.* **[25]**.

The method originated by Leibfried *et al.* was remarkably important at the NIST (National Institute of Standards and Technology) experiments of quantum tomography because a coherent displacement [Eq. (116)] can leave the state of the ions at many different locations of the phase space. This procedure is analogue to the motional-state technique previously described in (*Chapter 4.1.1*). It involves averaging measurements over different displacements via applying blue sideband pulses to an ion (with an internal state $|g\rangle$). Probability function with the form of Eq. (115) is recovered.

$$P_g(t,\alpha) = \frac{1}{2}\left\{1 + \sum_{k=0}^{\infty} Q_k(\alpha)\cos\left(\Omega_{k,k+1}t\right)e^{-\gamma_k t}\right\} \tag{146}$$

with $Q_k(\alpha)$ the population of a coherently displaced number state k.

5 Decoherence in trapped ions

Trapped-ions processes as described above are approximations of the real experiments where we have omitted any interaction with the environment. These couplings of the latter with the quantum system under study produce decoherence phenomena and the behaviour turning into a classical one. This constitutes one of the largest difficulties in quantum computing field. For this reason, quantum error-correction algorithms with high fidelity and fault-tolerance for information processing is one of the main developing topics currently.

5.1 Defect sources in ion trap quantum computers

The most relevant sources of decoherence in an ion trap quantum computer can be catalogued in three different categories: bit-flip error, dephasing and imperfect control of the system.

The first type of imperfections appears by radiation/absorption processes, generally spontaneous emission from the excited level. In bit-flip errors, some electrons are transferred of $|g\rangle$ to $|e\rangle$ states and viceversa. The presence of this error type is reduced because average life times of levels are some orders of magnitude longer than gate times.

Dephasing effects cause that a well characterized qubit (quantum system) follows a classical behaviour. In a two-level system, it leads to the creation of a relative phase between both states. The dephasing experimented is neither constant. It is generated by the fluctuations of a classical parameter such as the magnetic field which confines ions.

Magnetic fluctuations originate variations of the atomic resonance frequency. As a function of the change of the frequency over time they can be classified in fast fluctuations, if the relative phase varies during the experiment and in slow fluctuations, if it changes between experiments but remains constant throughout the same trial.

With the aim to reduce dephasing there exists many proposals. A generic way is to shield the ion trap from environmental magnetic fields with a high permeability metal. In addition, studying a Fourier analysis of the noise introduced by magnetic fluctuations it can be detected which are the main frequencies and synchronize them with the experiment phase evolution. Another interesting procedure is the use of ion levels with the same magnetic moment. Using this election, the dephasing evolution due to the magnetic field of the pair will be the same. The best choice is that state transition follows the form: $m_{F,g} = 0 \leftrightarrow m_{F,e} = 0$ which cannot feel linear Zeeman effect (it only experiences degeneracy breaks). Transitions between states can be induced with stronger magnetic fields which isolate higher order Zeeman phenomena. Nonetheless, the phase coherence between states is primarily important during phase gate operations (in two-qubit gates).

The last source of imperfections is originated by inefficiently calibrated parameters, as intensity of the laser beam fluctuations, or by side effects on the pulsed ion or surrounding ions.

The main imperfections caused on an ion trap computer are the following:

- *Pulse length errors*. The fluctuations are of an order below kHz. They emerge from laser pointing instabilities, intensity fluctuations or incorrect calibrations. An insufficient precooling increases the magnitude of these imperfections. However, when the number of ions inside the trap rises, this effect decreases because the Lamb-Dicke factor lowers when the number of ions increases **[26]**.

- *Detuning errors*. Its effect is the emergence of a constant phase evolution. It is produced by transition frequencies miscalibrations or when the time of coherent manipulations is considerably shorter than drift frequency fluctuations. The most effective method to minimize it is called *spin-echo method* **[27]**. It consists of swapping internal states of the qubit halfway. If the detuning is constant along all the experiment, it will be compensated after the complete manipulation time.

- *Addressing error*. When laser beams are focused in a single ion, residual illumination can interact with other ions. They produce uncontrolled unitary evolutions in the trap qubits. A methodology to reduce addressing at ions is the use of compound pulses. Splitting a large movement in the phase space into smaller ones entails that undesired evolution can be compensated. Another procedure to minimize addressing effects is to recalibrate trap stiffness to change the distance between ions **[28]**.

- *Off-resonant excitation*. In the same way that magnetic fluctuations can be Fourier characterized to identify main frequencies, they are not the only frequencies of the excitation. It is appreciable when a weak transition is driven next to a strong transition. This kind of excitation behaves as Rabi oscillations. Off-resonant terms modify the eigenvalues of the Hamiltonian, therefore, there are oscillations of the population to the new eigenstates. To increase accuracy, it is useful to use laser beams with no spectral Fourier components of the transition applied to the strong laser. If these excitements affect the qubit's phase they are called *AC-Stark shifts*

- Likewise bit-flip errors, when qubits are stimulated by Raman transitions, it has to be considered that they can spontaneous decay from the transition level between qubit states. This probability can be reduced applying large detunings **[29]**.

These are the most relevant imperfections that may occur in a trapped ion quantum computer. In practise, all of them can be minimized adjusting external parameters. However, a detailed study is needed to maintain simultaneously decoherence sources small.

5.2 Environmental quantum decoherence

On the other hand, other effects like the finite temperature of the ion string produce decoherence. To study them, the analysis of how the environment interacts with the system will be restricted

to the motion of a single atom, formally equivalent to a decoherence problem of a single mode of the EM field **[30]**.

With laser pulses, it is attainable to link motional and internal states of the qubit:

$$|g\rangle\,|n\rangle \longrightarrow \cos\theta\,|g\rangle\,|n\rangle + e^{i\phi}\theta\,|e\rangle\,|m\rangle \tag{147}$$

where $|n\rangle$ and $|m\rangle$ represents different motional states ($\langle n|m\rangle = \delta_{nm}$).

This kind of evolution is useful to characterize the system after measurements. Experimentally, laser fields are highly stronger than environment noise. However, the latter is not completely negligible. The global state can be understood as a coupling of $|n\rangle$, the motional states (which cannot be measured directly), $|\chi_M\rangle$, a quantum meter (the internal state) and, $|\phi\rangle$, the external environment.

$$|\Psi\rangle = (c_1\,|n\rangle + c_2\,|m\rangle) \otimes |\chi_M\rangle \otimes |\phi_e\rangle \tag{148}$$

The environment can be modelled as a superposition of states, $|\phi_e\rangle = \sum_k a_k\,|\phi_{e,k}\rangle$, where if the ion is strongly coupled to it, each state will attach to a different $|\phi_{e,k}\rangle$. Generally, environment states are unmeasured (because its evolution is hard to predict and control), it is assumed that they are barely correlated and $\langle\phi_{e,n}|\phi_{e,m}\rangle \approx 0$.

Coupling the superposed system with the meter leads to a dephasing at the motional states of the form $|n'\rangle = \exp(i\zeta_1)\,|n\rangle$. Consequently, after the second coupling the final state is

$$|\Psi_f\rangle = c_1\,|n'\rangle\,|g'\rangle\,|\phi_{e,1}\rangle + c_2\,|m'\rangle\,|e'\rangle\,|\phi_{e,2}\rangle \longrightarrow c_1\,|n\rangle\,|g\rangle\,|\phi_{e,1}\rangle + e^{i(\zeta_2-\zeta_1)}c_2\,|m\rangle\,|e\rangle\,|\phi_{e,2}\rangle \tag{149}$$

The information of the motional system states is represented by the density matrix. Considering the behaviour of the environment, the information relative to the off-diagonal is lost

$$\rho_f = |\Psi_f\rangle\,\langle\Psi_f| \approx |c_1|^2\,|n\rangle\,\langle n| \otimes |g'\rangle\,\langle g'| + |c_2|^2\,|m\rangle\,\langle m| \otimes |e'\rangle\,\langle e'| \tag{150}$$

It leads to search for methods to measure the coherence terms of the density matrix indirectly through internal states of the ion **[31]**.

Environmental decoherence can be modelled using reservoirs. In particular, a single ion can be studied as a harmonic oscillator system interacting with different types of reservoirs. They will be interpreted as a bath of quantum oscillators **[32]**. Based on the effect they produced in the qubit, two differentiated high-temperature reservoirs will be studied: amplitude and phase reservoirs.

They are important because in all experiments decoherence can be characterized as them. The temperature is associated with the lumped elements of the electrodes.

High-temperature amplitude reservoir Hamiltonian is:

$$H_{AR} = \frac{\hbar}{2} \sum_i \Gamma_i a b_i^\dagger + \text{H.c.} \tag{151}$$

with $a, a^\dagger$ ladder operators of the harmonic oscillator and $b, b^\dagger$ environment ladder operators. Γ_i establish the coupling strength.

A more theoretical analysis of the Hamiltonian was made by Murao and Knight, 1998 **[33]**. The following procedure is a suitable method to recreate this kind of decoherence in a laboratory in order to isolate the effect (and study it in controlled conditions).

The interaction is modelled as the coupling between the ion and a noisy electric field, $\underline{E}$. It is uniformly distributed amidst electrodes and it has some frequencies of the energetic motional spectrum of the ion. This situation is equivalent to a dipole (the ion) inside a classical electric field. Thus, the potential of the qubit is:

$$U = -\underline{p} \cdot \underline{E} = -Z|e|\Delta x \cdot E \tag{152}$$

where $Z|e|$ is the ion charge and Δx the separation from the equilibrium position.

The motional states utilized are coherent states, $|\alpha\rangle$ and $|\alpha'\rangle$ produced forming Schrödinger-cat states. The procedure tracked is: firstly, the state is exposed to the field a fixed time. Recombining the superposition obtained, the internal state is measured. In order to compare the decoherence evolution, the result is contrasted with the initial state **[34]**.

Results reveal that decoherence rate evolution is directly proportional to phase space separation $\Delta\alpha = |\alpha - \alpha'|$ of the superposition. Experimentally, there exist discrepancies with the model because the interaction of the environment and the system is negligible $|\phi_{e,1}\rangle \approx |\phi_{e,2,}\rangle \approx |\phi_e\rangle$ and the internal states are not influenced by $|\phi_e\rangle$. As the noise of the field can be classically measured without altering the ion, its effect can be reversed in artificial noise.

On the other hand, a high-temperature phase reservoir Hamiltonian is

$$H_{PR} = \frac{\hbar}{2} a a^\dagger \sum_i \Gamma_i b_i^\dagger + \text{H.c.} \tag{153}$$

This case cannot change the energy of the harmonic oscillator and it is used for modeling quantum non-destructive measurements **[35]**. It is studied tuning properly the trap frequency altering the phase evolution of the harmonic movement. Besides, a uniform Gaussian noise is applied below a frequency threshold smaller than the trap frequency (to avoid energy transference processes).

6 Conclusions

In this work, we have given an introduction to the quantum computing field. First of all, we have presented the mathematical formalism, including the most important quantum logic gates and an example of quantum algorithm.

Thereafter, we have described fundamentals of ion traps, a physical system where qubits can be implemented. More specifically, we have explained how ions behave inside the trap, its Hamiltonian and a way to precool the system in order to start computing at a known state with a high probability. The manipulation of ions inside the trap is made with laser pulses. For the purpose of quantum computing, the system must be inside Lamb-Dicke regime to decouple internal and motional states properly. The creation of quantum logic gates is achieved choosing an appropriate detuning to address ions. Single-qubit gates can be created with diverse sequences of laser field pulses. Two-qubit gates are formed in a similar way. To read the information, after the manipulation, we have to use one of the many methods proposed to recover the information of motional ions states. Experimentally, these processes are not ideal. The environment, among other things, e.g., imperfect detuning, has an important role in fluctuations which trigger decoherence phenomena (sources of error).

Nowadays, ion-trap quantum computers with 40 operating qubits have been achieved. However, the ultimate scope of this field is the creation of completely operative quantum computers. This poses many challenges to scientists due to the requirements of controlling and manipulating systems with high number of particles. Quantum computing in general, and with trapped ions in particular, may bring new tools for solving unaffordable problems at the moment like chemistry or engineering *ab initio* as well as the creation of new ”unbreakable” quantum cryptography models. Only the future can tell which developments the field will finally produce.

7 References

[1] SHOR, P.W., 1994. Algorithms for quantum computation: discrete logarithms and factoring. *Proceedings 35th Annual Symposium on Foundations of Computer Science*, 124.

[2] DIVINCENZO, DAVID P., 2000. The Physical Implementation of Quantum Computation *Fortschritte der Physik* **48**, 771-783.

[3] ASFAW A., CORCOLES A., BELLO L. AND BEN-HAIM Y. *et al.*. Learn Quantum Computation Using Qiskit, 2020. `http://community.qiskit.org/textbook`

[4] *Bloch sphere*, 2009. `https://en.wikipedia.org/wiki/Bloch_sphere#/media/File:Bloch_sphere.svg` (last accessed: June 12, 2021)

[5] NIELSEN, MICHAEL A. AND CHUANG, ISAAC L.. Quantum Computation and Quantum Information. Cambridge University Press, 2000.

[6] Physics with Trapped Charged Particles, 2015. `https://indico.cern.ch/event/315947/sessions/61194/attachments/606588/834751/Paul_traps_until_page_79.pdf` (last accessed: June 12, 2021)

[7] COOK, RICHARD J., SHANKLAND, DONN G. AND WELLS, ANN L., 1985. Quantum theory of particle motion in a rapidly oscillating field. *Phys. Rev. A* **31**, 564.

[8] MAJOR, FOUAD G, GHEORGHE, VIORICA N AND WERTH, GÜNTHER. Charged particle traps: physics and techniques of charged particle field confinement, 209-302. Springer-Verlag Berlin Heidelberg, 2005

[9] CIRAC, J. I., GARAY, L. J., BLATT, R., PARKINS, A. S. AND ZOLLER, P, 1994. Laser cooling of trapped ions: The influence of micromotion. *Phys. Rev. A* **49**, 421.

[10] LOUDON, RODNEY. The Quantum Theory of Light. Oxford: Clarendon, 1973.

[11] STENHOLM, STIG, 1986. The semiclassical theory of laser cooling. *Reviews of Modern Physics* **58**, 699.

[12] LEIBFRIED, D., BLATT, R., MONROE, C. AND WINELAND, D., 2003. Quantum dynamics of single trapped ions. *Review of Modern Physics* **75**, 281-324.

[13] MONROE, C., MEEKHOF, D. M., KING, B. E. AND WINELAND, D. J., 1996. A "Schrodinger" Cat Superposition State of an Atom. *Science* **272**, 1131.

[14] GERRY, CHRISTOPHER AND KNIGHT, PETER. Introductory Quantum Optics. Cambridge: Cambridge University Press, 2004.

[15] MØLMER, KLAUS AND SØRENSEN, ANDER, 1999. Multiparticle Entanglement of Hot Trapped Ions. *Phys. Rev. Lett.* **82**, 1835-1838.

[16] SØRENSEN, ANDERS AND MØLMER, KLAUS, 2000. Entanglement and quantum computation with ions in thermal motion. *Phys. Rev. A* **62**.

[17] SEPIOL, MARTIN. A high-fidelity microwave driven two-qubit quantum logic gate in 43Ca+. PhD diss. University of Oxford, 2016.

[18] CASANOVA, J., MEZZACAPO, A., LAMATA, L. AND SOLANO, E., 2012. Quantum Simulation of Interacting Fermion Lattice Models in Trapped Ions. *Phys. Rev. Lett.* **108**, 2.

[19] BENHELM, JAN, KIRCHMAIR, GERHARD, ROOS, CHRISTIAN F. AND BLATT, RAINER, 2008. Towards fault-tolerant quantum computing with trapped ions. *Nature Physics* **4**, 463.

[20] WILLIAMS, COLIN P., 2011. Explorations in Quantum Computing. *Texts in Computer Science*, 51-122.

[21] WALLENTOWITZ, S. AND VOGEL, W., 1995. Reconstruction of the Quantum Mechanical State of a Trapped Ion. *Phys. Rev Lett.* **75**, 2932.

[22] BARDROFF, P. J., C., LEICHTLE, G. SCHRADE, AND W. P. SCHLEICH, 1996. Paul trap multi-quantum interactions. *Acta Phys. Slov.* **46**, 1.

[23] LEIBFRIED, D., MEEKHOF, D. M., KING, B. E., MONROE, C., ITANO, W. M. AND WINELAND, D. J., 1996. Experimental Determination of the Motional Quantum State of a Trapped Atom. *Phys. Rev. Lett.* **77**, 4281.

[24] FREYBERGER, MATTHIAS, 1997. Probing the quantum state of a trapped atom. *Phys. Rev. A* **55**, 4120.

[25] BARRETT, M. D., CHIAVERINI, J., SCHAETZ, T., BRITTON, J., ITANO, W. M., JOST, J. D. AND KNILL, E., LANGER, C., LEIBFRIED, D., OZERI, R. *et al.*, 2004. Deterministic quantum teleportation of atomic qubits. *Nature* **429**, 737-739.

[26] WINELAND, D.J., MONROE, C., ITANO, W.M., LEIBFRIED, D., KING, B.E. AND MEEKHOF, D.M., 1998. Experimental issues in coherent quantum-state manipulation of trapped atomic ions. *Journal of Research of the National Institute of Standards and Technology* **103**, 259.

[27] HAHN, E. L., 1950. Spin Echoes. *Phys. Rev.* **80**, 580.

[28] REICHLE, R., LEIBFRIED, D., KNILL, E., BRITTON, J., BLAKESTAD, R. B., JOST,

J. D., LANGER, C., OZERI, R., SEIDELIN, S., WINELAND, D. J. *et al.*, 2006. Experimental purification of two-atom entanglement. *Nature* **443**, 838-841.

[29] OZERI, R., LANGER, C., JOST, J., DEMARCO, B., BEN-KISH, A., BLAKESTAD, B., BRITTON, J., CHIAVERINI, J., ITANO, W., HUME, D. *et al.*, 2005. Hyperfine Coherence in the Presence of Spontaneous Photon Scattering. *Phys. Rev. Lett.* **95**.

[30] SCHLEICH, WOLFGANG. Quantum optics in phase space. Berlin: WILEY-VCH, 2001.

[31] HAFFNER, H, ROOS, C AND BLATT, R, 2008. Quantum computing with trapped ions. *Physics Reports* **469**, 155-203.

[32] POYATOS, J. F., CIRAC, J. I. AND ZOLLER, P., 1996. Quantum Reservoir Engineering with Laser Cooled Trapped Ions. *Phys. Rev. Lett.* **77**, 4728.

[33] MURAO, M. AND KNIGHT, P. L., 1998. Decoherence in nonclassical motional states of a trapped ion. *Phys. Rev. A* **77**, 4728.

[34] MYATT, C. J., KING, B. E., TURCHETTE, Q. A., SACKETT, C. A., KIELPINSKI, D., ITANO, W. M., MONROE, C. AND WINELAND, D. J., 2000. Decoherence of quantum superpositions through coupling to engineered reservoirs. *Nature* **403**, 269-273.

[35] WALLS, D. F. AND MILBURN, G. J., 1985. Effect of dissipation on quantum coherence. *Phys. Rev. A* **31**, 2403.

[36] SHANKAR, R. Principle of Quantum Mechanics. 2nd Edition. Heidelberg: Springer Verlag, 1994.